

Coherent control of sub-terahertz confined acoustic nanowaves: Theory and experimentsN. D. Lanzillotti-Kimura,^{1,*} A. Fainstein,¹ A. Lemaitre,² B. Jusserand,³ and B. Perrin³¹*Centro Atómico Bariloche & Instituto Balseiro, C.N.E.A., R8402AGP S. C. de Bariloche, R. N., Argentina*²*Laboratoire de Photonique et de Nanostructures, C.N.R.S., Route de Nozay, F-91460 Marcoussis, France*³*Institut des Nanosciences de Paris, UMR 7588 C.N.R.S.—Université Paris 6, F-75252 Paris, France*

(Received 14 March 2011; revised manuscript received 1 August 2011; published 27 September 2011)

Recently it has been theoretically proposed that phonons could be used to store and process information. We report coherent control experiments on acoustic-phonon nanocavities in the sub-THz range and discuss the feasibility of using this system as a phononic memory. The nanocavities provide localized and monochromatic waves, two essential characteristics to work as memories and actuators. A writing-erasing-reading procedure based on the coherent generation, control, and detection of acoustic phonons using ultrashort light pulses is presented. The results are in agreement with numerical simulations using an implementation of a photoelastic model. Our results open the way to the practical realization of complex nano-optomechanical devices.

DOI: [10.1103/PhysRevB.84.115453](https://doi.org/10.1103/PhysRevB.84.115453)

PACS number(s): 78.67.Pt, 63.22.Np, 43.35.Gk, 07.10.Cm

I. MOTIVATION

The implementation of phononic memories and actuators constitutes a necessary step toward one of the most ambitious and fascinating goals of nanophononics:^{1,2} storing and processing information using phonons. The creation, storage, and retrieval of a phononic state in a nanostructure on demand, without corrupting the information it carries, is still an open and challenging problem.

Several devices based on incoherent phonons and heat transfer have been proposed and theoretically analyzed, such as thermal diodes,^{3–9} transistors,¹⁰ heat pumps,^{11,12} logic gates,¹³ and memories based on negative differential thermal resistances.¹⁴ Solid-state thermal rectifiers¹⁵ have also been experimentally studied.

Thermal devices work with broadband incoherent phonons and the frequency response is intrinsically limited by heat-transfer processes restricting their use to low-frequency applications. Coherent acoustic phonons in the GHz-THz range represent a viable alternative to rapidly actuate on nanodevices and modulate electronic, optical, and elastic properties. Recent reports showed that devices based on nanometric multilayers can be used to generate, detect, confine, and filter sub-THz acoustic phonons.^{1,16–20} The generation and detection of hypersound is usually performed using ultrafast light pulses in a pump-probe experimental scheme.²¹ By engineering the acoustic,²² optical,²³ and electronic properties²⁴ of the multilayered transducers it is possible to generate monochromatic phonon spectra.

Coherent control experiments have been extensively used to manipulate the destruction of excitons in quantum wells,²⁵ to manipulate chemical reactions,²⁶ to optimize energy conversion processes,^{27,28} etc. Using coherent control techniques it is also possible to create and annihilate coherent acoustic phonons in the fs-ps scale and within nanometric volumes. In the field of nanophononics, tailored pulse shapes (such as multiple pump pulses) have been used to control superlattice phonons,²⁹ surface acoustic waves,³⁰ phonons in photonic crystal fibers,³¹ and to generate high-frequency phonons using piezoelectric quantum wells.³²

In spite of all these advances in acoustic-phonon engineering the concept of phononic memories and actuators

based on ultrahigh-frequency acoustic phonons, to the best of our knowledge, has not been studied. In standard coherent phonon generation experiments, a first intense laser pulse impinges the sample generating a packet of phonons. These phonons modulate the optical properties of the structure, and thus modify its reflectivity. A second less-intense laser pulse measures the perturbed optical reflectivity as a function of the time delay between the pump and probe pulses. In this paper we present experimental results on the coherent control of acoustic nanowaves in the 500-GHz range. In contrast with previous investigations in this domain, we use nanocavities to provide localized and monochromatic waves, two characteristics that are essential for their use in memories and actuators. To study the nanocavity we set up a coherent control experiment based on one excitation laser pump pulse, one delayed control pulse, and a less intense probe pulse to sense the acoustic state of the cavity. We show that acoustic nanocavities based on semiconductor multilayers can potentially be used as solid-state phonon memories. Coherent phonons inside the cavity can be generated with the pump, annihilated with the control pulse, and measured within the lifetime by ultrafast pulses. Thus, by means of coherent control techniques acoustic nanocavities are capable of retaining information which can be written, erased, and read without destroying the stored state.

The paper is organized as follows: Section II introduces the experimental technique, sample design, and presents the experimental results; the simulations and theoretical analysis of the coherent control of acoustic phonons in nanocavities are addressed in Sec. III. Finally, Sec. IV is devoted to the discussion of the results and the conclusions.

II. COHERENT CONTROL EXPERIMENTS

Acoustic-phonon nanocavities^{17,33} using periodic superlattices as acoustic distributed Bragg reflectors (DBRs) have been recently studied as efficient monochromatic coherent phonon generators and detectors.¹⁸ The layer thickness and materials constituting the mirrors and the spacer of the nanocavity determine the resonance frequency.^{17,22,33} The number of periods in the DBRs and the acoustic impedance mismatch between the chosen materials determine the Q factor of the acoustic resonator.¹⁷ Under resonance conditions, the

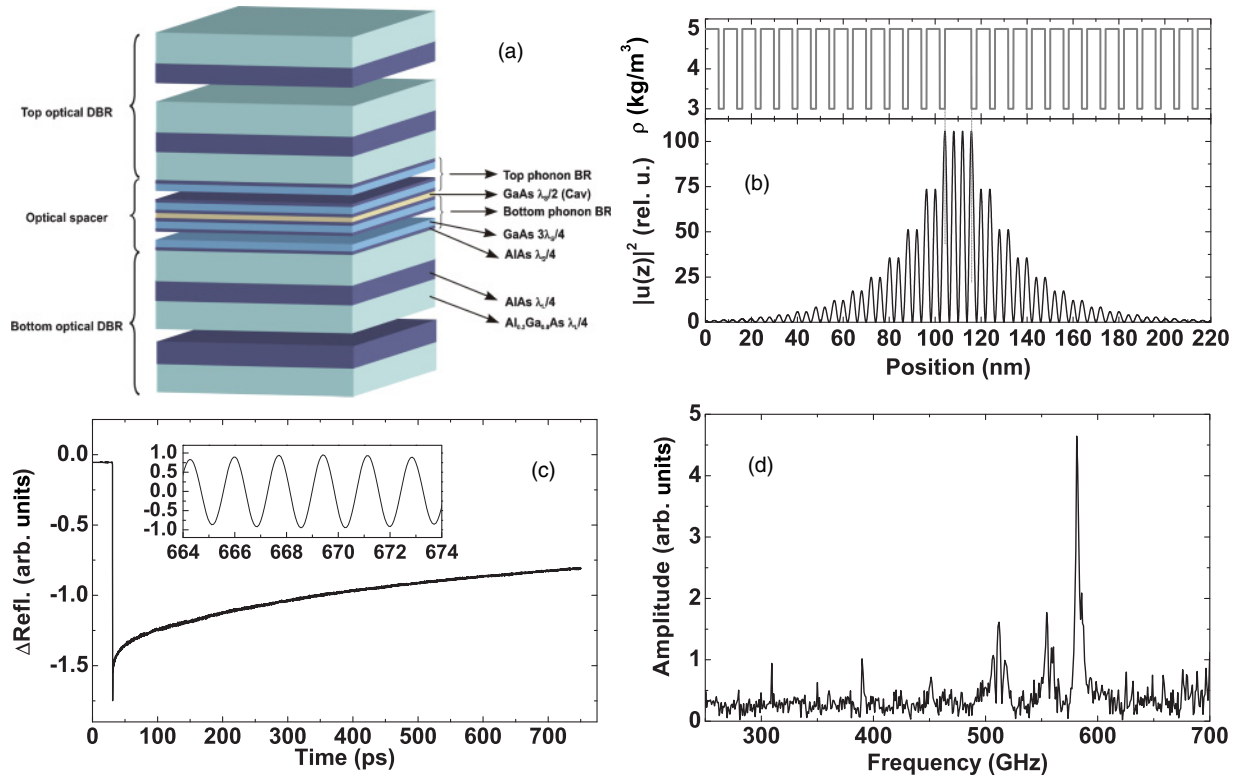


FIG. 1. (Color online) (a) Schematics of the studied sample formed by an acoustic nanocavity embedded in an optical microcavity. (b) Phononic field corresponding to the resonance frequency (580 GHz) as a function of the position in an acoustic nanocavity formed by two GaAs/AlAs-based mirrors enclosing a GaAs spacer. A mass density profile is include to identify the position of the acoustic spacer. (c) Time-resolved reflectivity measured in a standard pump-probe configuration. The inset show the filtered signal corresponding to the confined acoustic phonons. (d) Coherent phonon generation spectrum measured in the acoustic nanocavity. The experiment was performed at room temperature with the laser set at 790 nm, in resonance with the optical cavity mode.

phononic field is localized and amplified in the spacer of the nanocavity. Figure 1(a) shows the calculated phononic field for a 580-GHz acoustic nanocavity formed by two acoustic DBRs of 13 periods of GaAs/AlAs ($3\lambda_{ph}/4, \lambda_{ph}/4$), enclosing a $3\lambda_{ph}/2$ GaAs spacer. Here λ_{ph} is the resonance phonon wavelength in each material. The mass density profile is also included to facilitate the identification of the spacer layer. Note that the phononic field is localized mainly in the spacer, and penetrates into the DBRs. The penetration depth is determined by the acoustic impedance mismatch between the materials forming the mirrors. The cavity amplifies the strain intensity by a factor of ≈ 100 , and has a nominal Q factor of 500. In such acoustic nanocavity, phonons will be confined with a lifetime of ~ 1 ns, i.e., ~ 500 oscillation cycles. This number can reach 2000 by increasing the number of periods forming the DBRs.³⁴ Lattice anharmonicity does not affect essentially the Q factor of a phonon nanocavity of frequency ω_c , even at room temperature where $k_B T \gg \hbar \omega_c$.³⁴ Thus, memories and actuators based on confined coherent phonons can be operated at room temperature without being strongly affected. Acoustic nanocavities have been previously investigated in Raman scattering and coherent phonon generation experiments.^{23,35} When used as light-hypersound transducers in coherent phonon generation experiments, they are ideal sources of tailored quasimonochromatic acoustic phonons in the sub-THz range.^{18,22–24}

In the standard pump-probe configuration for coherent phonon generation,²¹ a first laser pulse generates the coherent phonons through electrostriction or a deformation potential mechanism.³⁶ Taking into account that the typical laser pulse duration is ≈ 100 fs, and the considered phonons have frequencies below 1 THz, the excitation can be assumed to be a delta in time. A second pulse, the probe, senses the instantaneous optical reflectivity of the sample. By varying the delay between pump and probe pulses, the time-resolved reflectivity can be measured. A Fourier transform of the time traces allows to recover the frequency components of the acoustic nanowaves modulating the optical reflectivity.

We performed pump-probe experiments using a Ti:sapphire laser delivering 80-fs pulses at 80 MHz. Both pump and probe were focused onto a $\sim 50 \mu\text{m}$ spot, and were cross polarized to improve the signal-to-noise ratio. The probe pulse was delayed using a mechanical delay line. The pump beam was modulated at 1 MHz using an acousto-optic modulator (AOM) in order to allow a synchronous detection using a lock-in amplifier. The studied acoustic resonator is embedded in an optical microcavity³⁷ [see the schematics in Fig. 1(b)]. The optical structure is formed by a top (bottom) DBR made of three (ten) periods of AlGaAs/AlAs ($\lambda_l/4, \lambda_l/4$), where $\lambda_l \sim 790$ nm is the optical resonance wavelength of the microcavity. The optical mirrors enclose the acoustic nanocavity that performs as the optical spacer. The sample was grown on a (001) GaAs

substrate by molecular beam epitaxy, producing sharp and planar interfaces at atomic level.

The experiments were performed at room temperature, with the central laser wavelength set at 790 nm, in resonance with the optical cavity mode. The optical microcavity has a twofold function: On the one hand, it amplifies the electromagnetic field and thus the generation efficiency; on the other hand, it modifies the selection rules in a way that the system is sensitive to detect exactly the same phonons that were created by the pump pulse.^{23,38,39} Time traces of 750 ps were taken and Fourier transformed to analyze the frequency components of the phonon spectrum. A typical time trace is shown in Fig. 1(c), where a fast change in the reflectivity is observed at $t = 30$ ps and is due to the electronic excitation of the sample. At this time, pump and probe pulses coincide in time and space. In the inset we show the signal without the slowly varying background where highly monochromatic oscillations can be identified. Figure 1(d) shows the Fourier transform of the derivative of the time trace. This spectrum is characterized by a very intense peak at 580 GHz, and two broad peaks at lower frequencies related to modes distributed in the superlattices acting as phononic mirrors. By adjusting the energy of the laser it is possible to get rid of these SL modes.²⁴ In our case this optimization was limited by the design of the optical microcavity. The full width at half maximum (≈ 20 GHz) of the cavity mode peak is mainly determined by the integration window. It is worth noting that in coherent phonon generation experiments such as the ones described in this section, the measurements are only sensitive to coherent phonons, and the observed lifetimes are then limited by only two factors: intrinsic lifetime (determined by the interface roughness and anharmonicity) and escape time from the cavity through the acoustic DBRs (determined by the number of periods in the mirrors).³⁴

The experiments previously described permit to study the confined-phonon dynamics in a nanocavity. To manipulate the trapped phonons in the structure, a coherent control scheme becomes necessary. The coherent control of acoustic phonons requires a first pump pulse that generates a phonon wave packet at a specific location in space and at a time $t = t_0$; a second delayed pump pulse (control pulse) to generate a second phonon wave packet at $t = t_0 + \tau$; and a third delayed (less intense) pulse that probes the optical reflectivity of the sample. The acoustic wave packets propagate in the structure with a characteristic sound group velocity v . If $\tau > d/v$ (where d is the spatial width of the acoustic pulse), then the two (pump and control) acoustic pulses are spatially separated. If τ is an odd number of acoustic phonon semicycles, the coherent part of the pump-probe signal will be zero. This fact does not imply, however, that the existing phonons have been annihilated by the control pulse. Simply, their added effect in the probe reflectivity cancels out. On the other hand, if $\tau < d/v$, the second wave packet will acoustically interact with the first one, and it can annihilate the existing phonons if the proper delay is achieved. An acoustic nanocavity is peculiar in the sense that it spatially and spectrally confines phonons and thus, for any value of τ , the second group of phonons will be localized in the same position as the first one, and can control it by changing the delay τ . Consequently, phonons will be indeed generated or annihilated, and not only their effects added on a given probe method.

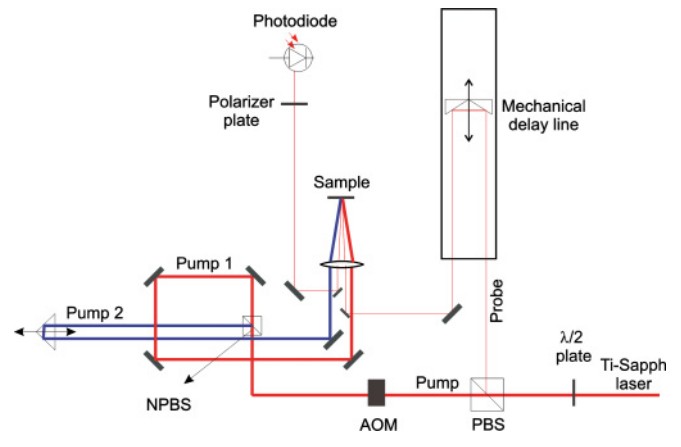


FIG. 2. (Color online) Setup of the coherent control experiments. The pump beam is divided into two pulses that are used to excite the sample. The probe pulse will sense the changes in the optical reflectivity induced by coherently generated phonons. AOM, PBS, and NPBS stand for acousto-optic modulator, polarizing beam splitter, and nonpolarizing beam splitter, respectively.

The schematics of the coherent control setup is shown in Fig. 2. A nonpolarizing beam splitter (NPBS) divides the original pump pulse into two identical pulses. A second mechanical stage controls the position of a prism used as retroreflector, and determines the delay between the pump and control pulses. The power of the two beams is regulated by neutral density filters (not shown in the schematics). The time delay between these two pulses is directly related to the phase between the phonons generated by the first and second pump pulses. The pump, control, and probe beams are focused onto a $\approx 50 \mu\text{m}$ spot of the sample using a single lens. The reflected probe beam is measured with a photodiode. Pump and probe beams are cross polarized to improve the signal-to-noise ratio by filtering the pump contamination using a polarizer plate in front of the photodiode. Figure 3 summarizes the experimental results of the coherent control of acoustic phonons confined in the nanocavity.

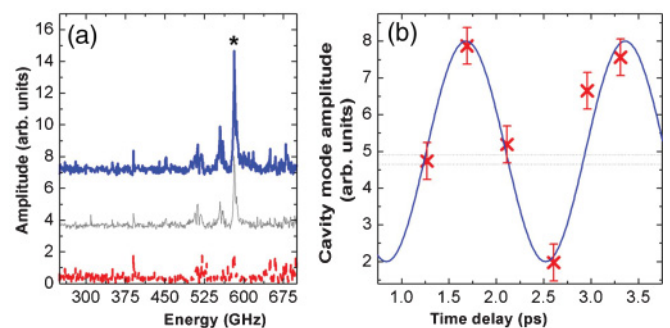


FIG. 3. (Color online) (a) Acoustic nanocavity spectra measured in the coherent control scheme with two pump pulses in phase (top, continuous line), two pump pulses in counterphase (bottom, dashed line), and with one pump pulse (middle, gray thin line). (b) Cavity mode intensity in the coherent control configuration as a function of the delay between the two pump pulses. Crosses correspond to experimental data, and the dotted line is a guide to the eye of the expected oscillatory behavior.

Figure 3(a) shows the acoustic nanocavity spectra obtained for the in-phase (continuous line) and counterphase (dashed line) conditions of the two pumps. A pump (probe) power of 20 mW (10 mW) for each beam was used. The peak at 580 GHz, indicated with an asterisk, corresponds to the confined acoustic phonons.⁴⁰ For comparison purposes, the spectrum corresponding to a single pump-pulse excitation is shown in gray. In all the cases the Fourier transform has been performed over a window of 700 ps after the arrival of the control pulse. Note that in the in-phase case the intensity doubles the value of the single pump experiment. On the other side, when the excitations are in counterphase, the intensity is almost annihilated. In Fig. 3(b) we show the intensity of the cavity mode (indicated with crosses) as a function of the time delay between the two pumps. The dotted line is a guide to the eye, to show the expected oscillatory behavior. The horizontal lines indicate the average intensity achieved individually by the two pumps in single excitation experiments. Note that maxima (minima) are obtained for delays equal to λ_{ph} and $2\lambda_{\text{ph}}$ ($\lambda_{\text{ph}}/2$ and $3\lambda_{\text{ph}}/2$).⁴¹

Using an ultrashort light pulse we impulsively generated coherent acoustic phonons in the nanocavity.^{18,22,23} The confined phonons remained in the cavity a characteristic time given by the Q factor of the acoustic resonator unless they are destroyed. With a second delayed pulse we were able to *annihilate* the existing phonons. The phononic state of the nanocavity was sensed with a less-intense probe pulse. From these experimental results we demonstrated that confined phonons in an acoustic nanocavity can be coherently created and annihilated. There are two essential characteristics to achieve full control of the acoustic phonons: (i) coherence and (ii) spatial confinement. The generated phonons are coherent since they were created by an impulsive excitation. In addition, they are confined in the cavity spacer due to multiple reflections in the acoustic DBRs.

III. THEORY OF THE COHERENT CONTROL IN CAVITIES

The described coherent control experiment represents the basis of a phononic memory, where the acoustic nanocavity stores the information. In the operation of the memory, it must be noted that (i) the acoustic phonons generated in the nanocavity are coherent, monochromatic and are spatially localized in the spacer of the structure: This is an essential condition to be able to annihilate them. Particularly, if the phonons are not localized, it is possible to generate two phonon wave packets in counterphase that could cancel the effects on the optical reflectivity—but the phonons are not annihilated. (ii) The Q factor of the resonator is finite, i.e., the phonons are continuously escaping to the substrate (note the similarity between an acoustic nanocavity and an electrical capacitor) and thus, the acoustic intensity within the spacer is varying with time. (iii) The efficiency of the second pulse to generate phonons will be determined by the electronic state of the sample at the arrival time of the second laser pulse; in other words, the capacity to efficiently annihilate the existing phonons can be optimized by a proper engineering of the control beam power.

To *write* a phononic state in the nanocavity, the best option is to create as many phonons as possible using a single pulse in the linear regime. To *erase* the phononic state, two factors must be taken into account: (i) the instant efficiency of the sample to annihilate the existing phononic state,⁴¹ and (ii) the quantity of phonons that are still localized into the cavity when the second pulse hits the structure. Failing to estimate these two factors could lead to the extreme case where phonons in counterphase are created when all the original phonons have left the resonator, resulting in a peak of counterphase-confined phonons.

In order to illustrate the dynamics of the acoustic phonons in a coherent control experiment, we performed numerical simulations of the generation process with an implementation of a photoelastic model using the standard transfer matrix for both the electric and the acoustic fields.⁴² The generated phonon spectrum G as a function of the phonon frequency (ω) is given by

$$G(\omega) \propto \int K(z)\eta(z,\omega)|E(z)|^2 dz, \quad (1)$$

where K , η , and E are the light-matter coupling constant (which is considered only material dependent), eigenstates of the strain in the structure, and electric field, respectively. The time evolution was computed as the inverse Fourier transform of the excitation spectrum

$$u(z,t) \propto \int G(z,\omega)\eta(z,\omega)e^{i\omega t} dt. \quad (2)$$

And in the case of a control pump pulse at $t = t_0$

$$u(z,t) \propto \int G(z,\omega)\eta(z,\omega)[e^{i\omega t} + e^{i\omega(t-t_0)}\Gamma(t_0)]dt, \quad (3)$$

where Γ is the Heavyside function. In Fig. 4 we show the results of the simulations. Brighter regions correspond to higher phonon intensities; side panels show the simulated detected time trace. Figure 4(a) corresponds to a single pump excitation at $t = 0$. The cavity spacer is located at ~ 110 nm, where an intense displacement can be observed. The intensity decays exponentially due to tunneling through the acoustic DBRs. The bright regions on both sides of the cavity spacer correspond to phonons generated in the acoustic DBRs that are not confined, and can rapidly escape to the substrate. In the side panel a constant amplitude signal can be observed in the full considered time window. Figure 4(b) shows the simulations results for the case of two-pump excitation, one at $t = 0$, and one (control) at $t = 162$ ps. This delay corresponds to 101 oscillations of hypersound with the cavity frequency. Under this condition, both pulses generate in-phase phonons, and thus an increase in the intensity of the confined phonons is achieved, as can be seen in the side panel. A relative delay of 100.5 oscillations will lead to an annihilation of the existing phonons; in Fig. 4(b) we illustrate this situation. After the control pulse impinges the sample at 161.2 ps, the intensity in the cavity spacer is almost null; a series of bright regions appear at both sides of the spacer, and they correspond to nonconfined modes that rapidly escape to the substrate. Since the relative delay between the first and the control pumps for these phonons is not an integer number of half-wavelengths, they do not interfere constructively or destructively; moreover, since the phonons generated by the first pump have already escaped into

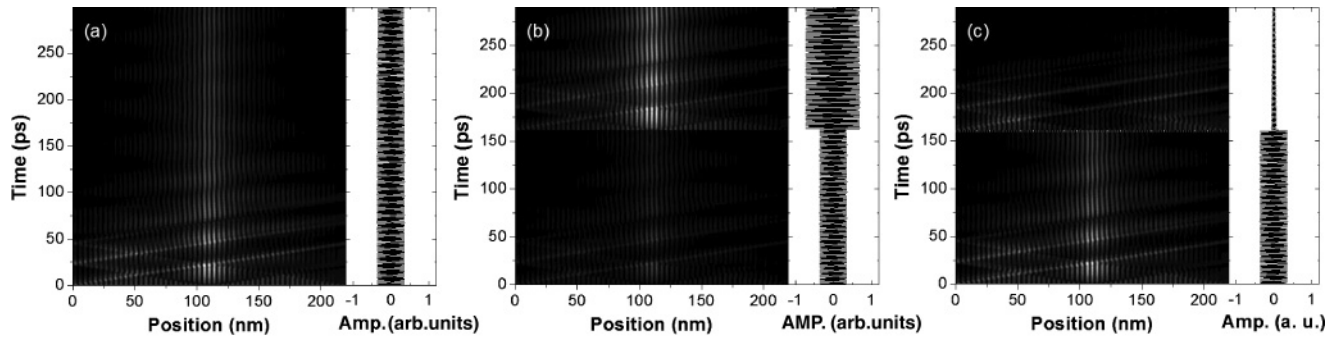


FIG. 4. Simulated time evolution of the generated coherent acoustic phonons in a coherent control setup. Brighter regions indicate higher phonon intensities. (b) The control pulse impinges the nanocavities at 162.0 ps, 101 phonon oscillation periods of delay, generating in-phase phonons. (c) The control pulses impinges the nanocavity at 161.2 ps, 100.5 phonon oscillation periods of delay, annihilating the previously existing confined phonons. Side panels show the simulated detected time trace corresponding to confined phonons in the cavity.

the substrate, they do not interact with the phonons generated by the control pulse. Observing the side panels, it is possible to foresee applications where a train of optimized optical pulses can keep the intensity of the signal constant, increase it, or annihilate the existing phonons in a feedback loop.

In technological applications, more than one bit can be necessary. Acoustic nanocavities can be concatenated^{43,44} to store multiple bits in a single monolithic structure. Coupled nanocavity structures present multiple confined modes that could be individually used and controlled to store phononic information. By a proper engineering of the electronic states of the structure and/or the laser pulse shape, the acoustic nanocavity modes could also be selectively excited and detected.²⁴

IV. DISCUSSION AND CONCLUSIONS

Acoustic excitations have already been used to modulate optical resonators, interferometers, electronic states, surface plasmons, etc.^{23,45,46} An acoustic nanocavity constitutes indeed the basis of a light-driven acoustic actuator. Such a device must comply with two requirements: (i) Phonons must be localized and amplified in order to effectively modify a system (e.g., excitonic levels, dielectric constants, phase transitions, etc.). (ii) There must be a mechanism to turn *on* and *off* the phonons, i.e., to control the actuator. In this way

a nano-optomechanical system can be actuated by confined acoustic phonons, and the actuator controlled by a series of ultrafast light pulses. In the cases studied in this paper, the controlled system is the optical confined mode of the microcavity: Its reflectivity is modulated if coherent phonons are present in the acoustic resonator. In addition, in this system, electromagnetic information can be stored in the acoustic resonator at room temperature for times in the nanosecond scale. This information can be written, recovered, and even modified while the acoustic phonons remain trapped in the cavity.

In conclusion, we have experimentally demonstrated the coherent control of sub-THz acoustic phonons trapped in semiconductor nanocavities, where the storage time is determined by the Q factor of the nanocavity. We presented a simple way to write, modify, and read a phononic bit using femtosecond laser pulses and a coherent control setup. Since the confined phonons are able to directly modulate photons, charge, or other excitations, the proposed phononic memory could also perform as an actuator in more complex nano-optomechanical devices.

ACKNOWLEDGMENTS

The authors acknowledge O. Mauguin and L. Largeau for the HRXRD characterization, and A. Miard for help in growing the sample.

*kimura@cab.cnea.gov.ar

¹N. D. Lanzillotti-Kimura, A. Fainstein, A. Lemaitre, and B. Jusserand, *Appl. Phys. Lett.* **88**, 083113 (2006).

²A. A. Balandin, *J. Nanosci. Nanotechnol.* **5**, 1015 (2005).

³M. Terraneo, M. Peyrard, and G. Casati, *Phys. Rev. Lett.* **88**, 094302 (2002).

⁴Baowen Li, Lei Wang, and Giulio Casati, *Phys. Rev. Lett.* **93**, 184301 (2004).

⁵Baowen Li, J. H. Lan, and Lei Wang, *Phys. Rev. Lett.* **95**, 104302 (2005).

⁶Dvira Segal and Abraham Nitzan, *Phys. Rev. Lett.* **94**, 034301 (2005).

⁷Bambi Hu, Lei Yang, and Yong Zhang, *Phys. Rev. Lett.* **97**, 124302 (2006).

⁸Dvira Segal, *Phys. Rev. Lett.* **100**, 105901 (2008).

⁹B. Liang, X. S. Guo, J. Tu, D. Zhang, and J. C. Cheng, *Nat. Mater.* **9**, 989 (2010).

¹⁰Baowen Li, Lei Wang, and Giulio Casati, *Appl. Phys. Lett.* **88**, 143501 (2006).

¹¹Rahul Marathe, A. M. Jayannavar, and Abhishek Dhar, *Phys. Rev. E* **75**, 030103 (2007).

¹²Dvira Segal and Abraham Nitzan, *Phys. Rev. E* **73**, 026109 (2006).

¹³Lei Wang and Baowen Li, *Phys. Rev. Lett.* **99**, 177208 (2007).

- ¹⁴Lei Wang and Baowen Li, *Phys. Rev. Lett.* **101**, 267203 (2008).
- ¹⁵C. W. Chang, D. Okawa, A. Majumdar, and A. Zettl, *Science* **314**, 1121 (2006).
- ¹⁶Ke-Qiu Chen, Xue-Hua Wang, and B. Y. Gu, *Phys. Rev. B* **61**, 12075 (2000).
- ¹⁷M. Trigo, A. Bruchhausen, A. Fainstein, B. Jusserand, and V. Thierry-Mieg, *Phys. Rev. Lett.* **89**, 227402 (2002).
- ¹⁸A. Huynh, B. Perrin, N. D. Lanzillotti-Kimura, B. Jusserand, A. Fainstein, and A. Lemaitre, *Phys. Rev. B* **78**, 233302 (2008).
- ¹⁹N. D. Lanzillotti-Kimura, B. Perrin, A. Fainstein, B. Jusserand, and A. Lemaitre, *Appl. Phys. Lett.* **96**, 053101 (2010).
- ²⁰N. D. Lanzillotti-Kimura, A. Fainstein, B. Jusserand, A. Lemaitre, O. Mauguin, and L. Largeau, *Phys. Rev. B* **76**, 174301 (2007).
- ²¹C. Thomsen, H. T. Grahn, H. J. Maris, and J. Tauc, *Phys. Rev. B* **34**, 4129 (1986).
- ²²N. D. Lanzillotti-Kimura, A. Fainstein, B. Perrin, B. Jusserand, A. Soukiassian, X. X. Xi, and D. G. Schlom, *Phys. Rev. Lett.* **104**, 187402 (2010).
- ²³N. D. Lanzillotti-Kimura, A. Fainstein, A. Huynh, B. Perrin, B. Jusserand, A. Miard, and A. Lemaitre, *Phys. Rev. Lett.* **99**, 217405 (2007).
- ²⁴M. F. Pascual Winter, G. Rozas, A. Fainstein, B. Jusserand, B. Perrin, A. Huynh, P. O. Vaccaro, and S. Saravanan, *Phys. Rev. Lett.* **98**, 265501 (2007).
- ²⁵A. P. Heberle, J. J. Baumberg, and K. Kohler, *Phys. Rev. Lett.* **75**, 2598 (1995).
- ²⁶A. Assion, T. Baumert, M. Bergt, T. Brixner, B. Kiefer, V. Seyfried, M. Strehle, and G. Gerber, *Science* **282**, 919 (1998).
- ²⁷Robert J. Levis, Getahun M. Menkir, and Hrschel Rabitz, *Science* **292**, 2598 (2001).
- ²⁸Herschel Rabitz and Regina de Vivie-Riedle, *Science* **288**, 824 (2000).
- ²⁹A. Bartels, T. Dekorsy, H. Kurz, and K. Kohler, *Appl. Phys. Lett.* **72**, 2844 (1998).
- ³⁰D. H. Hurley, R. Lewis, O. B. Wright, and O. Matsuda, *Appl. Phys. Lett.* **93**, 113101 (2008).
- ³¹G. S. Wiederhecker, A. Brenn, H. L. Fragnito, and P. St. J. Russell, *Phys. Rev. Lett.* **100**, 203903 (2008).
- ³²Cheng-Ta Yu, Kung-Hsuan Lin, Chia-Lung Hsieh, Chang-Chi Pan, Jen Inn Chyi, and Chi-Kuang Sun, *Appl. Phys. Lett.* **87**, 093114 (2005).
- ³³A. Huynh, N. D. Lanzillotti-Kimura, B. Jusserand, B. Perrin, A. Fainstein, M. F. Pascual-Winter, E. Perónne, and A. Lemaitre, *Phys. Rev. Lett.* **97**, 115502 (2006).
- ³⁴G. Rozas, M. F. Pascual Winter, B. Jusserand, A. Fainstein, B. Perrin, E. Semenova, and A. Lemaitre, *Phys. Rev. Lett.* **102**, 015502 (2009).
- ³⁵P. Lacharaise, A. Fainstein, B. Jusserand, and V. Thierry-Mieg, *Appl. Phys. Lett.* **84**, 3274 (2004).
- ³⁶An electrostrictive mechanism can be relevant if the excitation laser energy is below the electronic gap in semiconductors.
- ³⁷M. S. Skolnick, T. A. Fisher, and D. M. Whittaker, *Semicond. Sci. Technol.* **13**, 645 (1998).
- ³⁸N. D. Lanzillotti-Kimura, A. Fainstein, B. Perrin, B. Jusserand, L. Largeau, O. Mauguin, and A. Lemaitre, *Phys. Rev. B* **83**, 201103 (2011).
- ³⁹In infinite superlattices, the generated phonons by the pump pulse do not meet the selection rules of the detection process. In finite superlattices, the detection of these phonons relies on a residual overlap between the generated and detected spectra.
- ⁴⁰Using a resonant excitation it is possible to generate a monochromatic spectrum without side peaks (Ref. 24).
- ⁴¹As reported in Refs. 29 and 32, there is a saturation of the coherent generation amplitude for high pump powers corresponding to the saturation of the interband absorption. The results presented in Fig. 3 were obtained with powers well below this limit.
- ⁴²N. D. Lanzillotti Kimura, A. Fainstein, B. Perrin, and B. Jusserand, *Phys. Rev. B* **84**, 064307 (2011).
- ⁴³N. D. Lanzillotti-Kimura, A. Fainstein, C. A. Balseiro, and B. Jusserand, *Phys. Rev. B* **75**, 024301 (2007).
- ⁴⁴N. D. Lanzillotti-Kimura, A. Fainstein, B. Perrin, B. Jusserand, O. Mauguin, L. Largeau, and A. Lemaitre, *Phys. Rev. Lett.* **104**, 197402 (2010).
- ⁴⁵D. Moss, A. V. Akimov, O. Makarovskiy, R. P. Campion, C. T. Foxon, L. Eaves, A. J. Kent, and B. A. Glavin, *Phys. Rev. B* **80**, 113306 (2009).
- ⁴⁶M. M. de Lima, M. Beck, R. Hey, and P. V. Santos, *Appl. Phys. Lett.* **89**, 121104 (2006).